Direct current heating effects on Si(111) vicinal surfaces

2003 J. Phys.: Condens. Matter 15 S3255

(http://iopscience.iop.org/0953-8984/15/47/005)

INSTITUTE OF PHYSICS PUBLISHING JOURNAL OF PHYSICS: CONDENSED MATTER

J. Phys.: Condens. Matter **15** (2003) S3255–S3280 PII: S0953-8984(03)67519-3

Direct current heating effects on Si(111) vicinal surfaces

Hiroki Minoda

Department of Physics, Tokyo Institute of Technology, Oh-okayama, Meguro, Tokyo 152-8551, Japan

E-mail: hminoda@surface.phys.titech.ac.jp

Received 14 August 2003
Published 14 November 2003
Online at stacks.iop.org/JPhysCM/15/S3255

Abstract

Study on new types of step instability on a Si(111) vicinal surface induced by the direct current heating effect by reflection electron microscopy and optical microscopy is reviewed. One step instability is in-phase step wandering and the other is a periodic step density wave (PSDW). The former is due to electromigration of Si adatoms and steps are aligned in phase without changing mean step–step distance. This instability occurs at temperatures between 1000 and 1200 °C, under the step-down current heating condition. Steps are in the sinusoidal shape and their wavelength is in the micron order. The wavelength does not depend on the mean step–step distance or off-angle of the vicinal surface nor annealing time. The latter is induced by Au adsorption under step-down current heating at temperature between 830 and 930 °C where extremely straight step bands and Si(111) terraces are aligned periodically. The driving force of the PSDW is the modification of step structure due to electromigration of Au adatoms. These phenomena might be useful for micro-fabrication of surface from the industrial point of view as well as interesting from the fundamental point of view.

1. Introduction

Nano-scale control of structure of crystals is very important from the industrial point of view. Structure or morphology of a crystal surface is determined by the arrangement of surface steps. Control of an arrangement of the surface steps enables us to control surface morphology. Therefore, studies of structures and properties of surface atomic steps are very important from the industrial point of view and are also the basic science problems.

There are two ways to control arrangement of the surface steps or surface morphologies by self-organization. One is to use thermodynamic effects and the other is to use kinetic effects. One simple way to use thermodynamic effects is to modify surface free energy by adsorption of

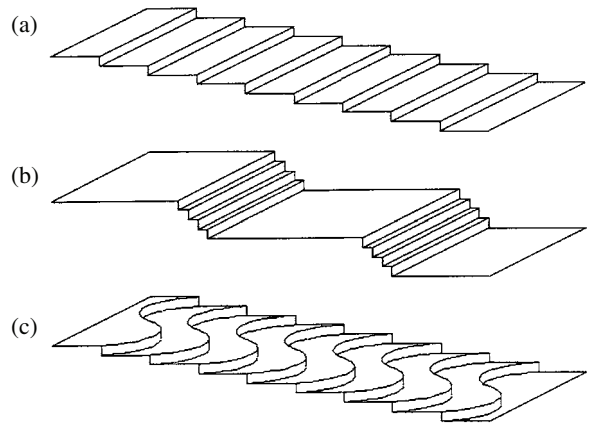

Figure 1. Three types of step arrangement on a vicinal surface: (a) regular array of steps (an R surface), (b) step bunching surface or surface with step bands (an SB surface) and (c) an in-phase step wandering surface (an IPSW surface).

foreign materials on the surface [1, 2]. The adsorption of foreign metal on a Si surface caused the formation of hill-and-valley structure composed of two stable facets. The dc-heating effect as well as homoepitaxial growth of Si can be used to control of surface morphology by kinetic effects [2, 3].

As illustrated in figure 1 there are three types of arrangements of the surface steps on a Si(111) vicinal surface obtained by dc-heating effect as described in the present paper. Figure 1(a) shows a regular array of single-height steps, which should be formed on annealed surfaces (hereafter denoted an R surface). Figure 1(b) shows a case where steps bunch to form step bands (SBs) and wide terraces in between (an SB surface). Figure 1(c) shows a case where steps wander in phase so as to make array of ridges and valleys on the surface. This kind of step wandering instability was recently found in our group and called in-phase step wandering (IPSW or an IPSW surface) [4]. These three step configurations are selectively obtained depending on the heating current direction and the temperature.

Transition between R and SB surfaces on a Si(111) vicinal surface by the dc-heating effect was found by Latyshev *et al* [3]. Figure 2 summarizes the dc-heating effects on clean vicinal Si(111) surfaces with small off-angles ($<1^\circ$). Above the phase transition temperature (around 830 °C) between the 1×1 and 7×7 structures there are four temperature ranges. In the temperature ranges I (830–1000 °C) and III (1180–1300)[Note 1] [3, 5], a step-up current heating gives an R surface and a step-down current heating gives an SB surface. On the other hand in the temperature ranges II and IV the dc-heating effect reverses and the step-up current gives an SB surface and the step-down current an R surface, and change of the heating current direction gives the reverse change between R and SB surfaces in all temperature ranges. Change of heating temperature also gives a reversible transition between SB and R surfaces. Reversal of the dc-heating effect takes place three times in the narrow temperature range of about 10–15 °C around the phase transition temperature between 7×7 and 1×1 [6][2].

One question in the dc-heating effect is the origin of a change of a step arrangement by a reverse of the heating current direction. The origin was explained by considering anisotropic migration of Si adatoms on the surface by external force of dc heating (surface

[1] There are discrepancies in the absolute values of these four transition temperatures in the literature. However, four ranges are commonly recognized.

[2] In this paper, directions $[\bar{1}\bar{1}2]$ and $[11\bar{2}]$ may be interchanged.

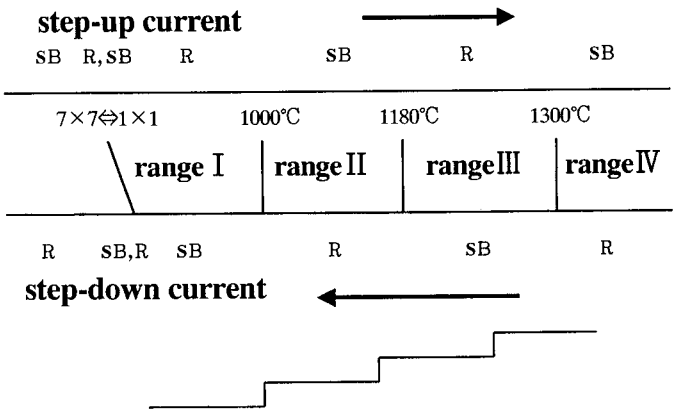

Figure 2. Temperature dependence of dc-heating effects observed on Si(111) surfaces with small off-angles (<1°). In the 1 × 1 phase, three transitions take place, giving rise to four temperature ranges I, II, III and IV.

electromigration). The driving force F acting on the atoms in the electromigration is expressed as

$$F = Z^* eE \tag{1.1}$$

where Z^*, e and E are the effective charge of adatoms, the elementary charge and the electric field on the surface, respectively [7]. The effective charge is generally divided into two parts (an electrostatic force part Z_{el} and a wind force part Z_{wind} due to momentum transfer from the carriers).

The anisotropic migration of adatoms due to the electromigration enhances or suppresses the deviation of terrace width distribution, and an SB surface or R surface is obtained depending on the heating current direction. The expression in equation (1.1) is applicable for surface electromigration of foreign metal adsorbed on a Si surface [7–14]. For foreign metals it is easy to investigate the sign of Z^* because foreign metals have different 'colours' from that of substrate Si and we can easily see the direction of migration of the metals. The sign of Z^* depends on the metal (some metal atoms migrate to the anode and others to the cathode) and in some cases it depends on the amount of deposit [7–14].

A second question is the origin of the three transitions in the 1 × 1 phase. The origin of the transitions has been extensively studied [3, 5, 15–32]. There are two main ideas to explain the three transitions. One is the change of the anisotropy or preferential direction of the migration and the other is the change of the mechanisms of the step bunching depending on temperature. It is difficult to know the sign of Z^* of the Si adatom because Si adatoms have the same 'colour' as the substrate and there has been no direct experimental evidence for the signs of an effective charge in the four ranges. Our recent study on the direction of migration of Si in the three ranges I–III [33] shows that the effective charge is positive in these temperature ranges and the change of the mechanisms of step bunching should be attributed to the transitions.

A third question is whether the dc-heating effects observed on low off-angle vicinal surfaces hold also on high off-angle vicinal surfaces, and whether the three transition temperatures between the four ranges depend on off-angle. There have been no systematic studies on these. Recently, we investigated the dc-heating effects on various kinds of clean Si(111) vicinal surface to answer this question [4, 34–41]. The results of these studies are introduced in the present paper [34–37].

In addition to the dc-heating effect on Si adatoms on clean Si(111) vicinal surfaces the dc-heating effect on foreign metal atoms on the surfaces is interesting [42–45]. As described above effective charge of the foreign metal atoms depends on the materials and surface structures on which metals migrate and some of the metals have negative effective charge. Thus, the small amount of foreign metal adsorption might modify the dc-heating effect on Si adatoms because adsorbed foreign metals might modify the sign or values of the effective charge of Si adatoms, the diffusion distance of the Si adatoms and step structure. These modifications might change the relationship between heating current direction and step arrangement (R or SB surface) or would change transition temperature. The arrangement of steps during Au deposition was observed, to investigate the effect of adsorption of foreign metal atoms on the dc-heating effect on the Si adatoms, and a new type of step instability was found by reflection electron microscopy (REM). In the present paper this new finding is also introduced [44, 45].

2. Experimental details

2.1. UHV electron microscopy and optical microscopy

An optical microscope (LEITZ-DMR) and a co-focal laser microscope (Lasertec 1LM21W with a Nikon Optiphot attached) were used for studies of large scale surface topography of IPSW. The co-focal microscope was used to investigate profiles of the surface and the optical microscope was used to observe the top view of the surface morphology. Although these optical methods have poor spatial resolution, the obtained results are consistent with the results obtained by using higher spatial resolution such as REM [38] and STM [35] (STM results were obtained in collaboration with Professor E D Williams' group at the University of Maryland). Some examples of STM images are presented for discussion of the initial processes of the change of the surface morphology.

For observations of surface structures and surface dynamics, an ultra-high vacuum (UHV) electron microscope was used [46]. The observations were performed by REM and reflection high energy electron diffraction (RHEED), which was reviewed in [47]. A ray diagram in the REM is shown in figure 3. An incident electron beam with a grazing angle gives rise to a RHEED pattern, and the REM image is formed from one or a few reflections in the RHEED pattern. Since the surface is seen with a small glancing angle, REM images are foreshortened along the imaging beam direction. Although the resolution is poor along the electron beam direction, the foreshortening allows us to observe wide areas along that direction.

2.2. Samples

Two types of sample were made as shown in figure 4. Panel (a) shows a rectangular shaped sample cut from a wafer with a size fitted to each apparatus. Wafers of Si(111) vicinal surfaces with various off-angles were used. Panel (b) shows a sample with a cylindrical groove on a (111) surface. The heating current was fed parallel to the longer side of the sample (perpendicular to the cylindrical groove axis) and the dc-heating induced step instability can be seen simultaneously on step-up and step-down current regions with various off-angles (0°–14°).

Samples were chemically cleaned, rinsed and mounted on the sample holder. The sample holder was introduced into the UHV chamber for long annealing or UHV microscopy and degassed by ac passing through at 600 °C. After degassing, the sample was flash heated at 1200 °C for cleaning. The temperature was measured by an optical pyrometer.

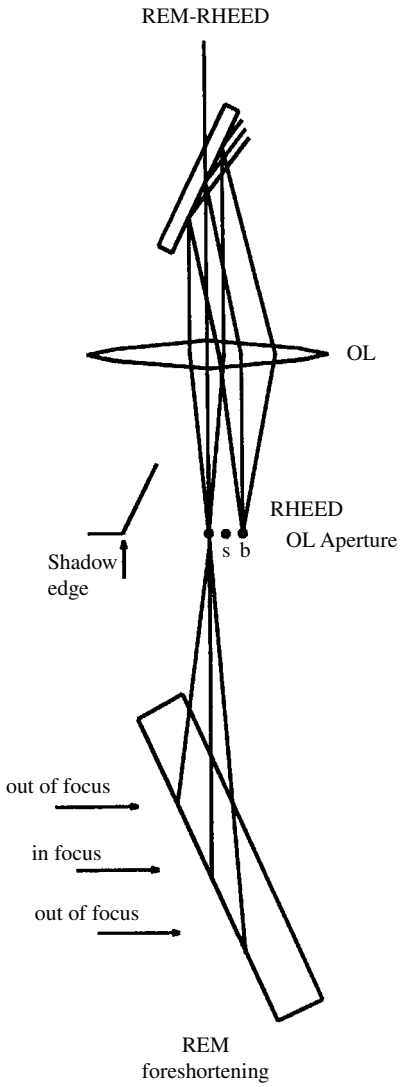

Figure 3. A ray diagram of REM–RHEED. In the reflection mode surfaces of bulk samples are observed with small glancing angles and the images are foreshortened by factors of 40–50 (note different scale marks along the beam direction and perpendicular to it in figure 20).

3. In-phase step wandering instability

3.1. General features of step instabilities

As described above, the step configuration on a Si(111) vicinal surface depends on the heating current direction and substrate temperature [2, 4, 36]. In this section general features of dc-heating induced step instabilities are reviewed. Figure 5 reproduces optical microscope images which show surface morphology on a surface of a sample with a cylindrical groove as shown in figure 4(b). Images were taken after dc annealing for (a) 127 h at 900 °C (range I), (b) 24 h at 1100 °C (range II) and (c) 3 h at 1250 °C (range III). Each image is composed

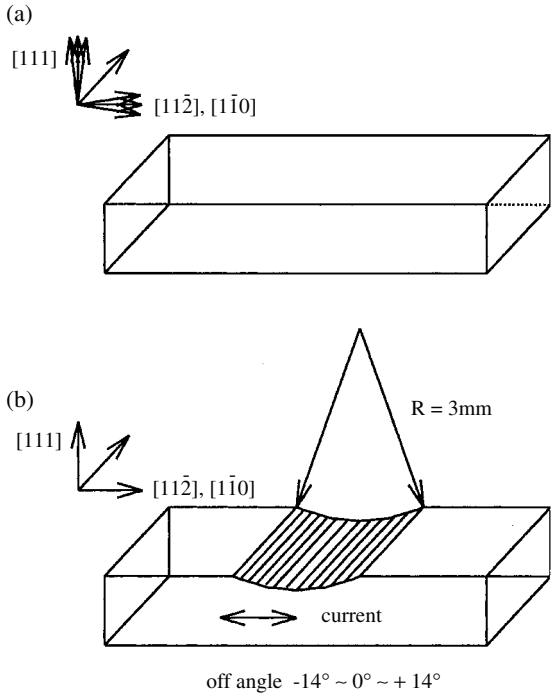

Figure 4. Two types of sample used for studies of dc-heating effects and adsorption induced step bunching and faceting. (a) A sample cut from a wafer with the proper orientation for studies. (b) A (111) oriented sample with a cylindrical groove whose surface has vicinal surfaces with off-angles from 0° to about 14°.

of more than ten micrographs taken with magnification of 200×. A scale mark of 200 μm is shown in each image. Arrows with letters 'I' indicate the heating current directions and the [$\bar{1}\bar{1}$2] crystallographic orientations are also indicated. Black downward arrowheads and open arrowheads at the top of the each image indicate positions of edges and the centre of the cylindrical groove of the samples, respectively. Surfaces at the centres of the grooves are in the (111) orientation. The vertical line images indicated by an arrow in (a) seen in the step-down current regions (the left-hand side of the groove) are giant step bands (SBs or SB surfaces) that are formed by step bunching after long annealing. The step-up current regions on the right in (a) are seen to be smooth (regular array of steps: R surfaces) except for scratch images formed on the surface during mechanical grinding. From (a) it is concluded that the step are bunched even on surfaces with large off-angles (∼14°). When the current direction was reversed, similar images showing the same dc heating effect were observed, which means that asymmetry along the [$\bar{1}\bar{1}$2] direction does not qualitatively influence the dc-heating effect.

Figure 5(c) of the sample annealed in range III shows similar features to those in (a): SB surfaces in the step-down current regions and R surfaces in the step-up current regions. Wider terraces between SBs in (c) in comparison with those in (a) are due to the longer surface diffusion distance of Si adatoms at higher temperature. It is concluded again that the dc-heating effect holds for large off-angle surfaces in range III.

Surfaces seen in (b) are quite different from those in (a) and (c). SBs of vertical lines are seen in the step-up current regions in the right-hand side of the groove (short segmented horizontal line images between the SBs will be discussed later). A reversal of the current

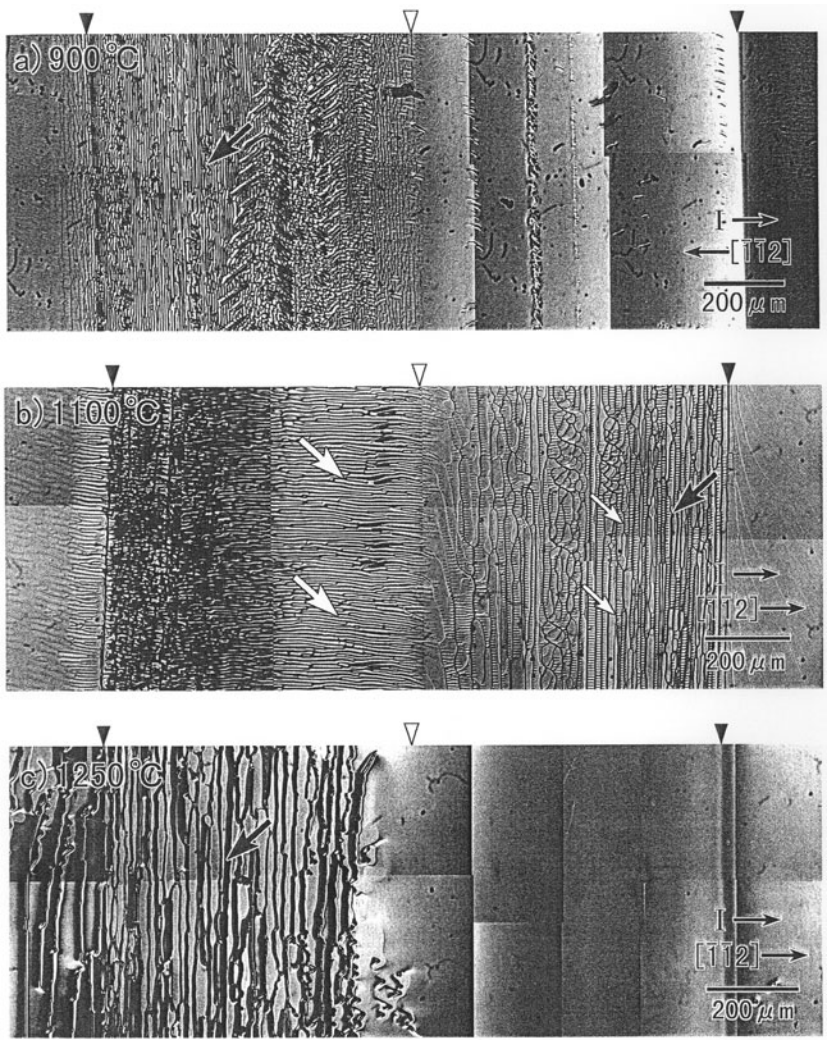

Figure 5. Optical microscope images showing surface morphology on a surface of a sample with a cylindrical groove taken after dc annealing for (a) 127 h at 900 °C in range I, (b) 24 h at 1100 °C in range II and (c) 3 h at 1250 °C in range III. In (a) and (c) step bunching in the step-down current regions indicated by black arrows and in (b) step bunching (black arrow) and IPSW of anti-bands (small white arrows) in the step-up and IPSW (large white arrows) in the step-down current regions are noted.

direction for step bunching in range II from those in ranges I and III is apparent, and dc-heating induced step bunching also occurs on the vicinal surface with large off-angle in range II. It is concluded that the general feature of dc-heating induced step bunching instability observed on vicinal (111) surfaces of small off-angle also holds for large off-angle surfaces up to 14° where an averaged single-height step separation is much smaller than the diffusion distances of adatoms on the (111) surface terraces.

A notable fact in (b) is that horizontal lines with a nearly equal spacing (more than a few microns) are seen in step-down current regions of the surface or the left-hand side of the groove. So far, a step-down current has been considered to cause an R surface. The horizontal

lines are concluded to be due to IPSW as shown in figure 1(c). This shows that step-down current in range II induces IPSW but an R surface. Another notable fact is that in the step-up current regions short segmented horizontal lines with spacing smaller than that in the step-down current regions are also seen between the SBs. The short segmented horizontal lines are also due to the IPSW. Although Bales and Zangwill [48] theoretically predicted IPSW instability due to the Schwoebel effect during homoepitaxial growth, IPSW instability under drift force on adatoms was not theoretically predicted. Wandering instability of an isolated step under drift force was predicted by Uwaha and Sato [19] and recently Suga *et al* [29] could show IPSW instability under a step-down drift force in the diffusion limited regime. Diffusion of adatoms along the steps with the help of step-down drift force was considered to enhance wandering of the steps. Sato *et al* [49] also showed IPSW instability under a step-down drift force in the case of permeable steps. However, the wandering kinetics has not been elucidated yet.

Figure 6 shows a high magnification optical microscope image of SBs formed by step-up dc heating (to the right in the figure) in range II. Bright vertical bands are SBs where surfaces are inclined to the left. Dark bands (indicated by sets of three small arrows) just on the right-hand side of the SBs are anti-bands (ABs) [50, 51], where surfaces are inclined to the right (see figure 7(c)). Between two adjacent SBs finger patterns pointing out to the right are seen as indicated by large arrows. The finger patterns are the well grown IPSW of ABs ($\mathrm{IPSW_{AB}}$). It should be noted that in AB regions the heating current is 'effectively' in the step-down direction as in the regions of IPSW (left-hand side of the groove in figure 5(b)).

Figure 7 schematically shows a sequence of changes of step configuration during step-up dc heating in range II: an R surface, an SB surface, an SB surface with AB and an SB surface with $\mathrm{IPSW_{AB}}$. At first, steps are bunched by step-up current heating as in (b). SBs and SB–SB separation grow and ABs start to form in (c). Finally the ABs are wandering in phase to form $\mathrm{IPSW_{AB}}$ as in (d) and $\mathrm{IPSW_{AB}}$ regions expand to form finger patterns.

There is a question of whether the phenomena on the cylindrical surface where the off-angle continuously changes (figure 5) are similar to those on vicinal surfaces with uniform off-angle. Studies on flat surfaces with various off-angles and at various temperatures showed that the answer to the question is yes. Examples for a 2°-off sample (from the (111) orientation to the $[11\bar{2}]$ direction) in range II at 1100 °C are shown in figure 8. Panel (a) shows the surface annealed by step-up current and panel (b) shows the surface annealed by step-down current. Patterns due to SB and $\mathrm{IPSW_{AB}}$ are clearly seen in panel (a) and patterns due to IPSW are seen in panel (b). The example shows the results for the case of the $[11\bar{2}]$ step but there are also similar results for cases of $[1\bar{1}0]$ and $[\bar{1}\bar{1}2]$ steps. One difference was that SBs along the $[11\bar{2}]$ directions are wavy due to the anisotropy of SB energy. These facts indicate that the current induced step behaviours are nearly isotropic and not strongly affected by step–step interaction.

3.2. A 'phase diagram' of the step instabilities

From figure 5, it is concluded that the dc-heating induced step instabilities as shown in figures 1 and 7 are observed on vicinal surfaces with off-angle up to 14°. As a next step, the off-angle dependence of the transition temperature was investigated [36]. With this aim we performed a heating experiment of the groove sample at several temperatures and figures 9 and 10 show the optical microscope images showing surface morphology on a sample with a cylindrical groove after dc heating at 950 and 1200 °C, respectively.

Figure 9 shows the surface of the sample after dc heating for 78 h at 950 °C (range I in figure 5). The edges and the centre of the groove are indicated by downward arrowheads in the figure. The current was fed to the right as indicated. As seen in enlarged images (b) and (c)

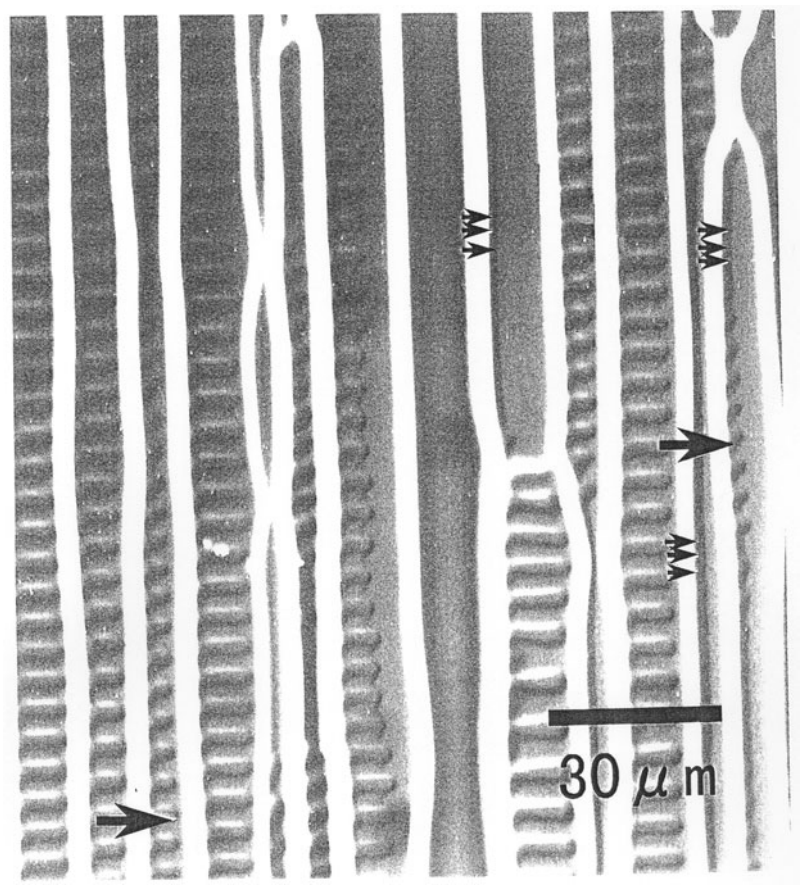

Figure 6. A high magnification optical micrograph showing SBs, and ABs and IPSW of ABs. The surface steps up to the right and was formed by a step-up dc heating.

characteristic features of range I (step bunching in the step-down current and the R surface in the step-up current regions) are only seen near the bottom of the groove. As seen on the left-hand side of images (a) and (b), IPSWs are seen in the step-down region with off-angles larger than 2°. In the step-up region (right-hand side of image (a) and more clearly in (d)) steps are bunched in the regions with off-angles larger than 11°. Both of the characters (IPSWs in the step-down region and SBs in the step-up regions) are observed in range II and this shows that character in range II is seen in the large off-angle regions and that in range I is seen in the small off-angle region. Thus, the transition temperature between ranges I and II depends on the off-angle of the vicinal surface, and the transition temperature on the vicinal surface with large off-angle is lower than that on the surface with small off-angle.

Figure 10 shows the surface of the sample after dc heating for 4 h at 1200 °C (at temperature in range III but close to the transition temperature between ranges II and III for the vicinal surface with small off-angle). Near the bottom of the groove (small off-angle regions) a step-bunching pattern (SBs and ABs indicated by arrows in (b)) is noted in the step-down current regions and R surfaces are seen in the step-up current regions, which is characteristic to range III. In large off-angle regions IPSWs and step bunching with $IPSW_{AB}$ (as seen in (c))

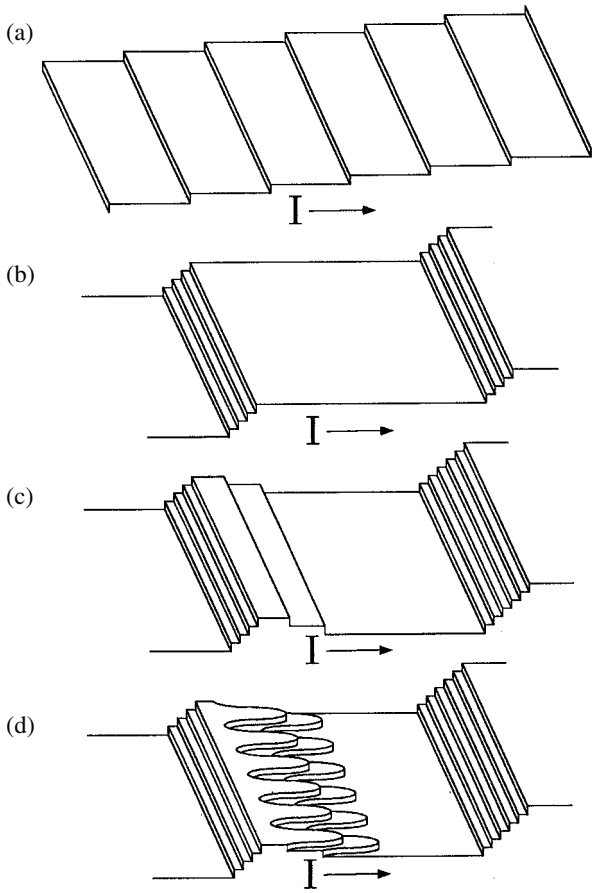

Figure 7. A schematic drawing showing a sequence of changes of step configuration during step-up dc heating in range II: an R surface, an SB surface, an SB surface with AB and an SB surface with $IPSW_{AB}$.

characteristic to range II are seen. Thus, an off-angle dependence of the transition temperature of step instability due to dc heating is evident.

Overall step instabilities were summarized in figure 11 [36], which was obtained from similar experiments as in figures 9 and 10 and from experiments using flat samples with a proper off-angle. R, SB, AB, IPSW and $IPSB_{AB}$ represent step configurations as described before. Though the boundaries are marked as solid lines, there are ambiguities in angles and temperatures. The boundary between ranges III and IV was not studied. The following three points are noted.

(1) Step instability is off-angle dependent. Range II is wider for large off-angle surfaces than for small off-angle surfaces.
(2) IPSW and $IPSW_{AB}$ are only seen in range II which means that range II is qualitatively different from ranges I and III.
(3) The boundaries are asymmetric for step-up and step-down current, which means that R and SB are not always counterparts of each other for dc-heating induced step instability for large off-angle surfaces.

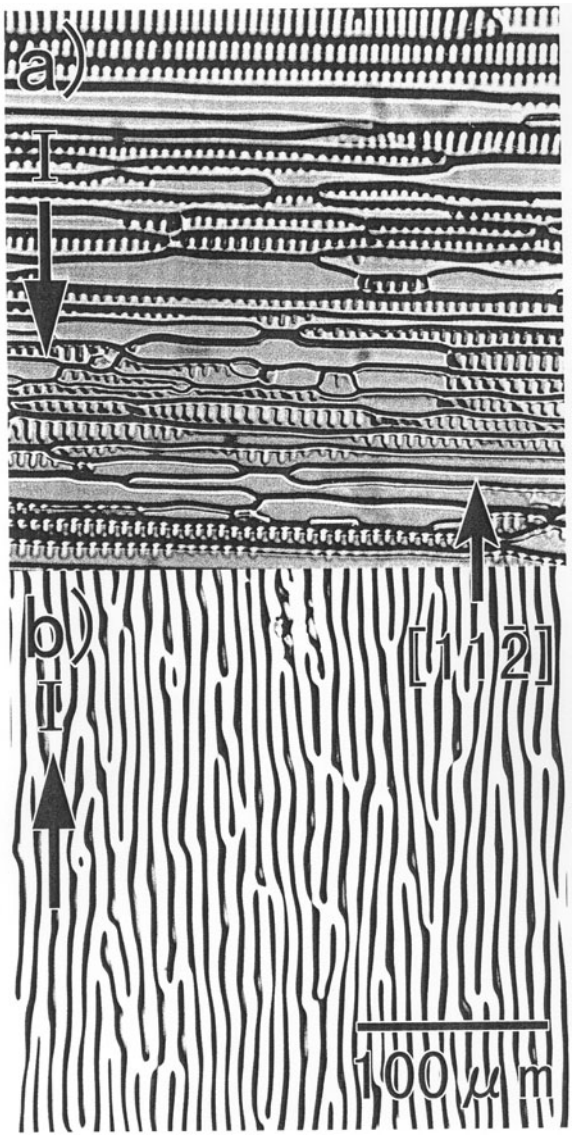

Figure 8. Examples for a 2°-off surface (from the (111) orientation to the [11$\bar{2}$] direction) taken after dc annealing at 1100 °C in range II.

3.3. Time evolution of IPSW

Previously we investigated the time evolution of dispersion of terrace width between successive single-height steps at initial stages of step bunching by *in situ* REM [52]. Terrace widths $d(t)$ during the bunching process as a function of time t after the reversal of heating direction have been measured and dispersion of the widths

$$\sigma^2(t) = \sum_i^N (d_i(t) - \bar{d})^2 / N\bar{d}^2 \qquad (= C(T, I, \bar{d})t) \tag{3.1}$$

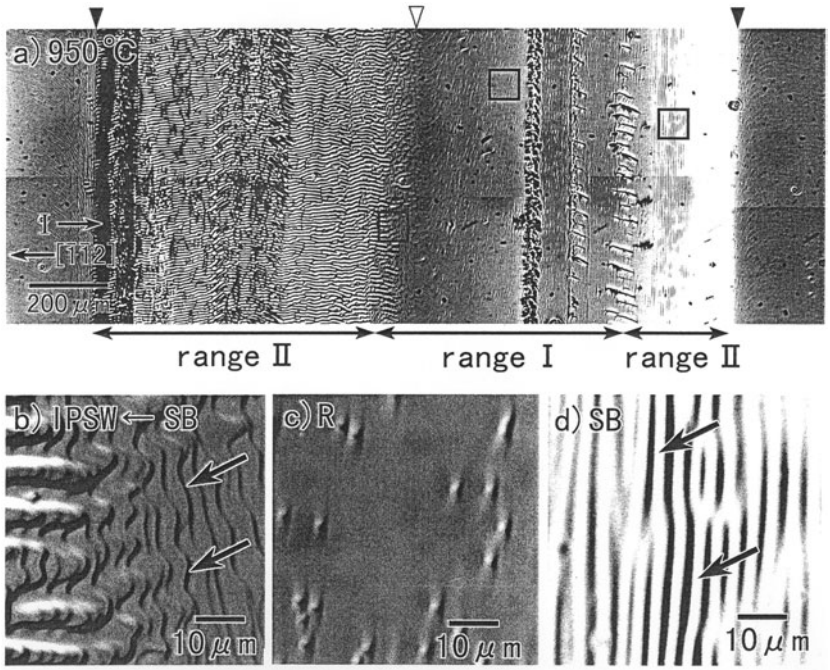

Figure 9. Optical microscope images showing a surface of the sample with a cylindrical groove after dc annealing for 78 h at 950 °C (range I) (a) and its enlarged images (b)–(d). IPSW (range II) and SB (range I) surfaces in step-down current regions and R (range I) and SB surfaces (range II) in step-up current regions are seen, which clearly shows that the boundaries between ranges I and II depend on the off-angle of the vicinal surface.

was calculated. It was found that time evolution of the dispersion is linear, as shown in the round brackets in equation (3.1), at the initial stage of step bunching, and a simulation showed a linear increase of the dispersion at the initial stage [52, 16]. It was found that the slope C depends on the temperature, current (experiments under different currents keeping the sample at the same temperature were carried out with use of an additional indirect heating method) and mean terrace width before the bunching. It was noted that (1) the slope is smaller for large mean terrace width $\bar{d}$ and (2) the slope is smaller for a smaller current.

Another parameter which has been recently studied is the maximum slope of SBs (β) during the bunching process [26–28]. The scaling law for the maximum slope of SBs was theoretically predicted for permeable and impermeable cases. The experimental studies showed that scaling factor depends on temperature and this suggests that the permeability of steps depends on the temperature [30, 53].

We have investigated the time evolution of IPSW patterns during dc heating. A series of optical microscope images of 5°-off samples which shows time evolution of IPSWs induced by dc heating is shown in figure 12 [35, 37]. In each panel the annealing time is shown at the upper left. Small regions of short segmented fringes with low contrast are seen in (a). They are regions where IPSW has been nucleated. In (b), vertical lines that are parallel to the heating current direction as shown in (c) appear all over the surface. Some parts of the lines have relatively high contrast. The stronger contrasted regions must be areas where nucleation of the IPSW has taken place. The contrast of the lines becomes lower and uniform in (c) after 8 h dc heating. These features indicate that the IPSW is formed by nucleation and expansion

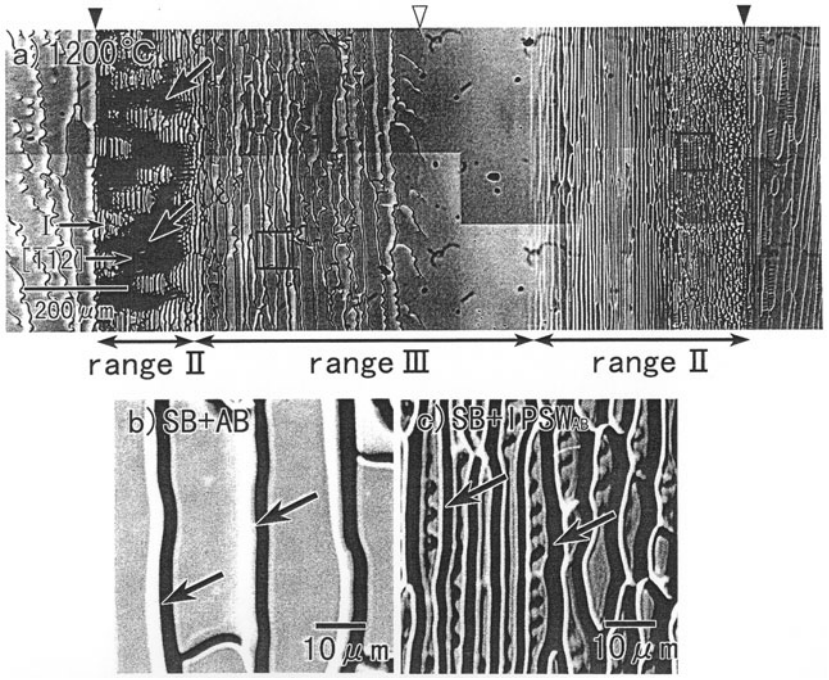

Figure 10. Optical microscope images showing a surface of the sample with a cylindrical groove after dc annealing for 4 h at 1200 °C (at temperature in range III but close to the transition temperature between ranges II and III) (a) and its enlarged images (b) and (c).

of the nucleated IPSW, which suggests that the IPSW instability is a non-linear effect. The weak fringes in (a) around the nucleated areas have the same period as that at the centre, which suggests that the period is governed by long range interactions. Since nucleation of IPSWs takes place all over the surface without correlation of their phases, branches of ridges or valleys of IPSWs should be formed when two wandering regions meet. These branches are commonly seen on the surfaces (see also figure 5). Further annealing from (c) to (f) causes increases of depth of the valleys (growth of amplitude of wandering steps), resulting in increased contrast of fringes.

Figure 13 shows wide area STM images of a 0.1°-off sample taken (a) before and (b) after 4 h dc heating at 1050 °C [35]. Panel (a) shows a nearly regular array of straight steps. Panel (b) shows that the position with large wandering amplitude corresponds to the ridge and clearly shows a nucleated IPSW. Image (b) is reproduced in a way that the vertical direction is magnified by a factor of two so as to enhance wandering of the steps. Surfaces in (a) and (b) step down to the bottom, and marks A and B show a nucleated ridge and a neighbouring ridge formed by less wandering steps. An enlarged inset (scale corrected image) shows two screw dislocations terminated at the surface, which suggests that they do not act as a trigger for nucleation of IPSWs. This suggests that nucleation starts from formation of ridges. However, nucleation at contaminants was also noted, where pinning of step motions during sublimation also caused ridge nucleation.

An IPSW on vicinal surfaces is characterized by the period (or wavelength) λ of wandering and the amplitude A of the sinusoidal form of steps as shown in figure 14 which shows the plan-view and cross-section of an IPSW along B–B′. When we used the sample of a vicinal

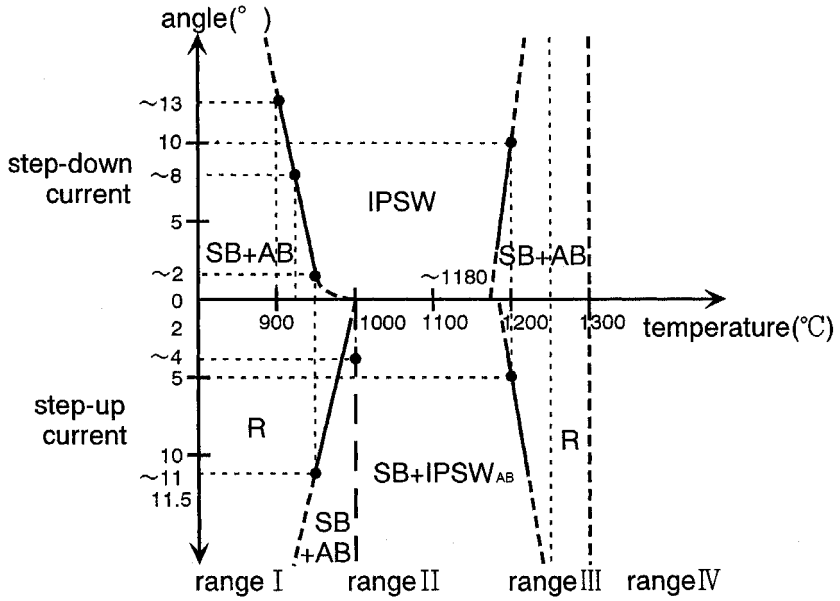

Figure 11. A 'phase diagram' of dc-heating induced step instability on Si(111) vicinal surfaces. The off-angle dependence of step configuration is clearly seen. The transition temperature between ranges III and IV has not been studied.

surface whose mean terrace width is $\bar{d}$, the amplitudes A can be evaluated by measuring the depth D of the valley from the ridge. The relationship between two values can be described as $2Ah/\bar{d} = D$ where h is step height (∼0.31 nm). The depth D was measured by using an optical method. The period λ was analysed by taking the Fourier transform of the optical microscope images.

Studies of the time evolution of IPSWs on various off-angle surfaces (1°, 2°, 3°, 5° and 11.5°) heated at 1100 °C were carried out [37]. One thing in the time evolution of the IPSW that should be pointed out is that the time required for nucleation of the IPSW and that to cover a whole surface (the stage shown in figure 12(c)) is shorter for smaller off-angle surfaces. As described later the formation process of the IPSW pattern is divided into three: the nucleation process, expansion process and growth process. An above-mentioned finding suggests that the step–step interaction plays important roles for nucleation and expansion of nucleated IPSWs. The details will be discussed later.

Figure 15 shows the plots of the time evolution of the period $\lambda(t)$ or wavelength of the IPSW pattern on various off-angle surfaces heated at 1100 °C. The period $\lambda(t)$ does not depend on the annealing time or the off-angle (for off-angles of 1°–5°), and is about 7 μm. The 11.5° off-angle surface showed an anomalously large period of 10 μm, which was attributed to facet formation [37]. The fact that the period induced by the dc-heating effect does not depend on the annealing time or off-angles is the most important finding in this study. This suggests that the period of the IPSW is a very good observable because the period of the IPSW does not strongly depend on the experimental conditions. We can use any off-angle of the vicinal surface and we can choose any annealing time for quantitative study of IPSWs. The quantitative study of the IPSWs is more effective than step bunching for investigation of surface electromigration in this system.

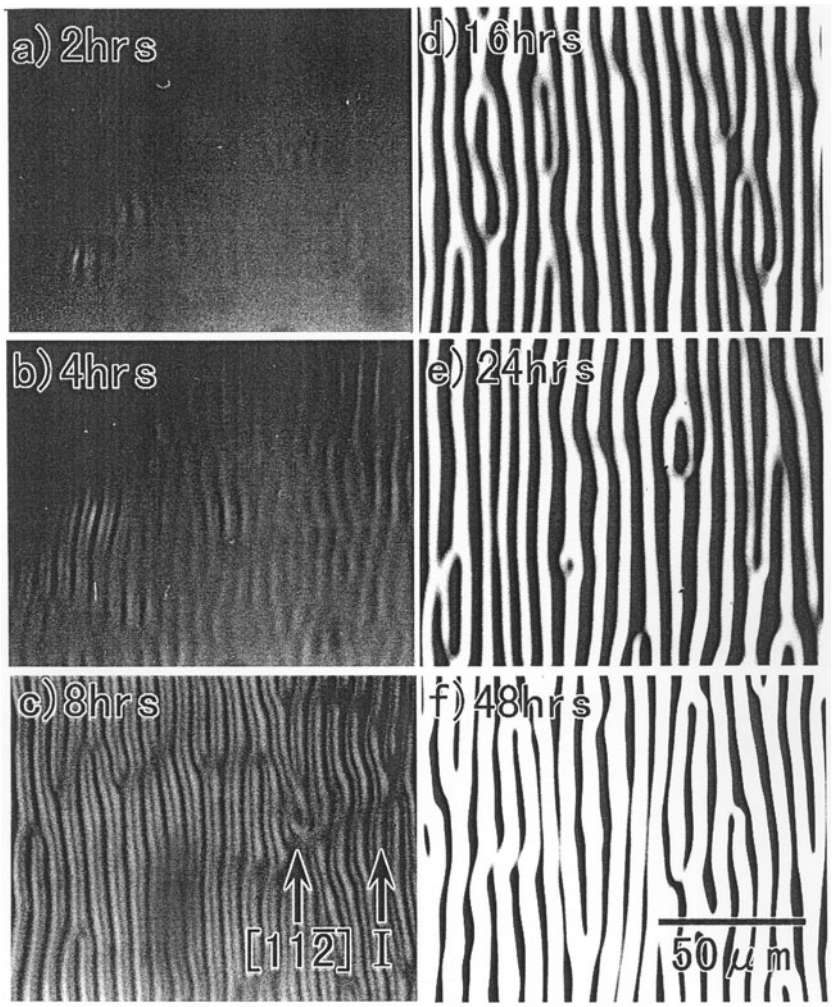

Figure 12. Optical microscope images which show time evolution of IPSWs on 5°-off samples by dc annealing for 2–48 h at 1100 °C. Nucleation and growth of IPSW regions from (a) to (c) and an increase of depth of valleys from ridges (contrast changes) from (c) to (f) are seen.

The time evolution of the amplitude $A(t)$ for surfaces with off-angle less than 5° is reproduced in figure 16. From figure 16 we can find two things.

(1) Amplitude increases non-linearly and grows as $t^{1/2}$ for annealing time t and seems to saturate at around 24–48 h. This growth feature is expected from the theoretical study by Natori and Suga [54]. This fact together with the fact that onset of the IPSWs is in a nucleation manner strongly suggest the non-linear feature of IPSWs.
(2) Saturated amplitude A_s depends on off-angle ($A_s(\theta)$, or $A_s(\bar{d})$) and is larger for smaller off-angle surfaces. However, the saturated values of depth D are smaller for smaller off-angle surfaces. The larger saturated amplitudes for the smaller off-angle surfaces also suggest roles of the step–step interaction in control of the saturated amplitude.

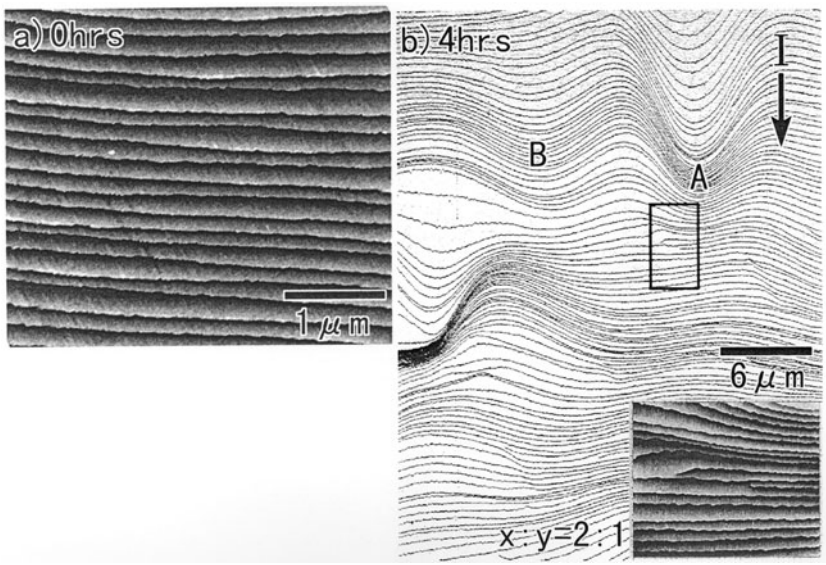

Figure 13. Wide area STM images of a 0.1°-off sample taken (a) before and (b) after 4 h dc annealing at 1050 °C. In-phase wandering of individual steps is seen near at the nucleation regions of the IPSW.

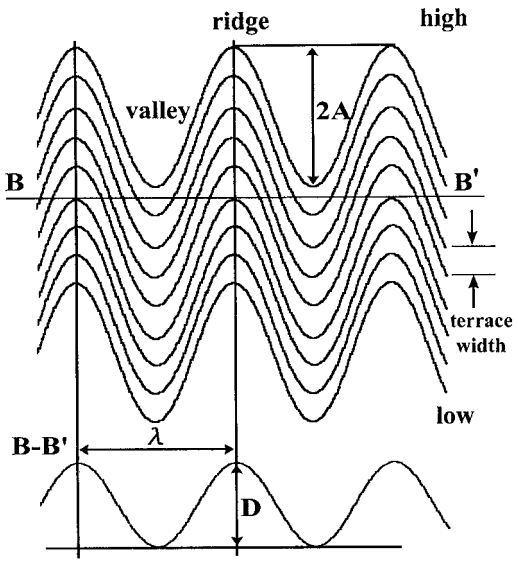

Figure 14. A schematic drawing of an IPSW and its surface profile with parameters period λ, amplitude A and mean step distance $\bar{d}$, which characterize the IPSW. There is a geometrical relation among the depth D of valleys from the ridges, amplitude A, mean terrace width $\bar{d}$ and step height h: $2Ah/\bar{d} = D$.

3.4. Effect of drift force component parallel to the mean step direction

So far, the IPSW was studied when the heating current (drift forces on adatoms) was perpendicular to the mean step direction. Effects of drift force component parallel to the

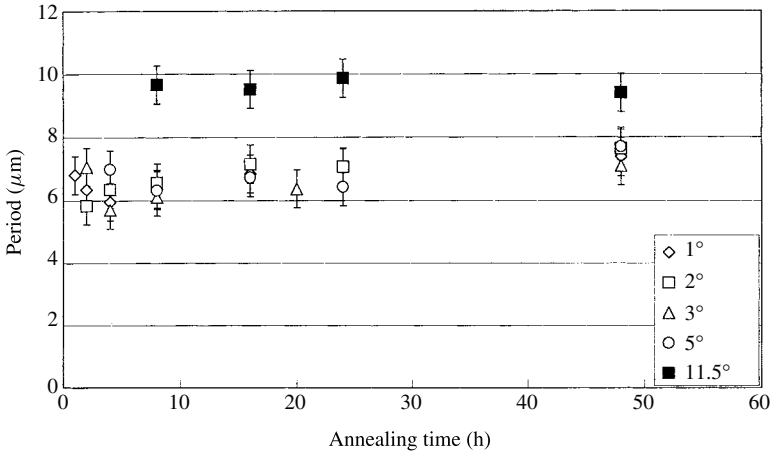

Figure 15. Time evolution of the period $\lambda(t)$ of IPSWs for various vicinal surfaces (off-angles are 1°, 2°, 3°, 5° and 11.5°) annealed at 1100 °C. The period $\lambda(t)$ does not depend on the annealing time or the off-angle except for a 11.5° off-angle surface and is about 7 μm.

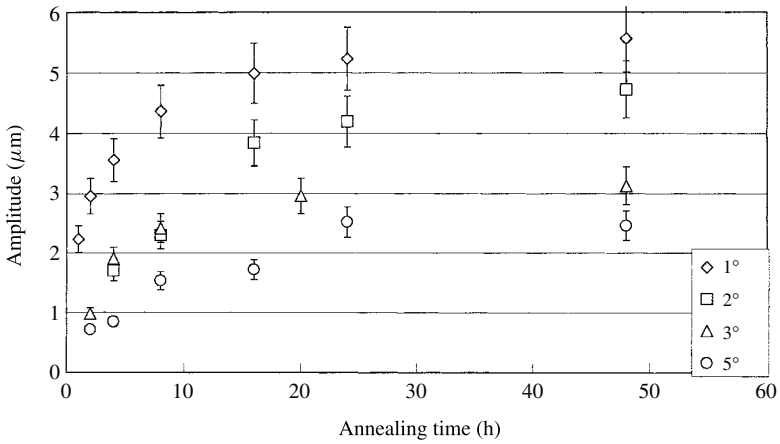

Figure 16. Time evolution of amplitude of IPSWs for various vicinal surfaces (off-angles are 1°, 2°, 3° and 5°). Amplitudes grow faster at the initial stages and saturate after 24–48 h dc heating. Amplitude is larger for smaller off-angle surfaces due to smaller step–step repulsive interaction.

mean step direction were studied by feeding the heating current inclined from the step-down direction [34]. Optical microscope images of 5°-off samples taken after 24 h dc heating at 1100 °C are shown in figure 17. The angle at the upper left in each micrograph shows the inclination angle from the step-down direction toward the clockwise direction. All the images are reproduced in such a way that the step-down direction in each image is upward. From panels (a)–(h), angles ϕ_0 between the step-down direction and the current direction (indicated by arrows in the centre panel) were 0°, 60°, 90°, 150°, 180°, −120°, −90° and −30° respectively.

From panels (a) and (e), it is noted that steps are bunched for step-up current heating and the IPSW pattern is formed for step-down current heating, respectively. When a step-up current component exists as in panels (d) and (f), steps are bunched and IPSWs of anti-bands are seen in between step bands. The directions of ridges and valleys of $\mathrm{IPSW_{AB}}$ are parallel to

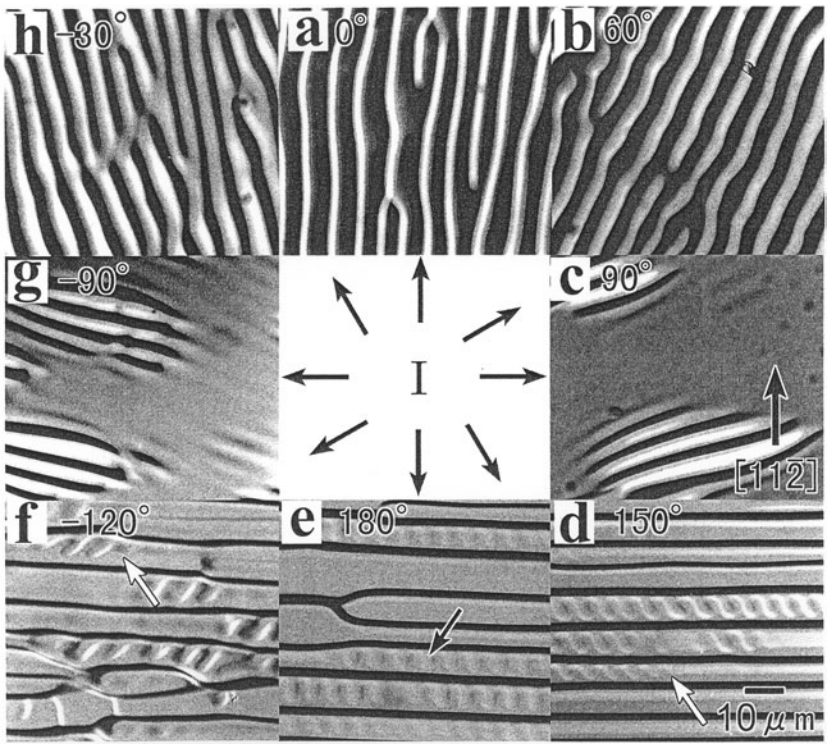

Figure 17. Optical micrographs of 5°-off surfaces taken after dc heating for 24 h at 1100 °C. Direct current direction was varied for each panel as shown by arrows in the centre panel. Note that directions of ridges and valleys are not parallel to the current direction in panels (b) and (h), while they are parallel to the current direction in panels (d) and (f).

the current in (d) and (f). On the other hand, when a step-down current component exists as in (b) and (h), the IPSW pattern is formed but the ridges and valleys are in the directions between the current and step-down directions. IPSW patterns are also formed when the heating current direction is parallel to the steps as in panels (c) and (g).

Figure 18 reproduces a series of optical microscope images of the 5°-off surface taken after various dc heating times at 1100 °C for $\phi_0 = 60°$. All the images are reproduced such that the current direction is upward and the step-down direction is in the upper-left direction as shown in (a) where the R surface before dc heating and an IPSW surface expected when the current is in the step-down direction are schematically illustrated. After 3 h annealing (b), nucleation of IPSW regions is seen and the directions of ridges and valleys are close to the step-down direction. One of the notable differences between figures 18 and 12 is that it takes a longer time for the IPSW pattern to cover the whole surface (it takes about 6 h in the present case as in figure 18(c) and about 4 h in the previous case as in figure 12(b)). This delayed time for nucleation and expansion of the IPSW pattern in figure 18 is attributed to a smaller current component in the step-down direction (a smaller drift force). Another fact to be noted in figure 18 is reorientation of ridges and valleys as seen from (b) to (f). Panel (f) taken after 48 h dc heating shows areas where ridges and valleys are nearly parallel to the current direction at a place indicated by a circle. These facts suggest that the current component parallel to the mean step direction does not affect the nucleation of the IPSW but affects the growth and expansion of the IPSW. At the initial stage when amplitudes of the IPSW are very small, the step–step

distance should be shortest in the direction perpendicular to the steps. The effect through the step–step interaction should be apparent in the direction perpendicular to the mean step direction. Thus, this fact suggests that propagation of the wandering pattern occurs through the step–step interaction rather than drift force.

Figure 19 schematically shows changes of step arrangement observed in figure 18. The current is decomposed to $I_\perp$ (component perpendicular to the mean step direction) and $I_\parallel$ (component parallel to the mean step direction). Nucleation of IPSW regions where ridges and valleys are parallel to the $I_\perp$ direction is shown in (a). The delayed time of nucleation of IPSW regions is considered to be caused by a smaller $I_\perp$ value than in the case of $I_\perp = I$ as mentioned above. Reorientation of the IPSW pattern corresponds to an increase of angle ϕ shown in figure 19(b) from zero (the stage shown in (a)) to ϕ_0 (that in (c)). $I_\parallel$ induces a phase shift between neighbouring wandering steps because $I_\parallel$ causes atom drift parallel to the steps (drift to the right in the case of figure 19). Thus, migration of adatoms to the step-down direction on the left-hand side of a ridge should be more than that on the right-hand side of it. This asymmetric diffusion field pushes protruding parts (which form ridges) of the steps towards the $I_\parallel$ direction (to the right in the case of figure 19) or dented parts (which form valleys) of the steps opposite to the $I_\parallel$ direction. This is consistent with the phase shift of an isolated wandering step due to the drift force component parallel to the step [34].

4. Periodic step density wave

So far, the dc-heating effect on Si adatoms on a Si(111) vicinal has not been reviewed. In this section the dc-heating effect on foreign metal atoms, which was recently found, is briefly introduced [44, 45]. Figure 20 reproduces two series of REM images during Au deposition on the 5°-off surface at 860 °C. Series A ((a)–(d)) is taken during Au deposition for step-up current heating and another series B ((e)–(h)) is taken for step-down current heating. The electron beam direction for imaging is shown by a white arrow in (a). The foreshortening factor of these images is approximately 1/40. Images (a) and (e) which show initial surface morphology are seen in homogeneous contrast, which means that surface steps are arranged regularly (mean terrace width is approximately 3 nm). Each surface step is not resolved under these imaging conditions. Bright and dark areas seen in (b)–(d) and (f)–(h) are step free and step band areas, respectively. Thus, both series show step bunching processes. The adsorption rate of Au was about 0.1 ML min^{-1} and step bunching started when approximately 0.3 ML of Au (a critical coverage) was adsorbed.

Although step bunching takes place on the whole surface for both cases, the aspects of the bunching processes are quite different. For step-up current heating the step bunching pattern is quite similar to that commonly observed when steps are bunched on clean Si(111) vicinal surfaces by electromigration of Si adatoms. On the other hand the bunching pattern in series B for step-down current heating has a periodic structure. The extremely straight step bands and (111) terraces are regularly arranged and there are few branches of the step bands. The periodic array of step bands (periodic step bunching or periodic step density wave, PSDW) as seen in series B has not been observed and this is a very interesting new finding. Another thing that should be pointed out is that this periodic pattern is formed by composition of metal adsorption (thermodynamics) and surface electromigration (kinetics) effects as described below. This shows a new possibility to control surface morphology or step configuration by composition of multiple effects.

Transition between the usual step bunching pattern and the PSDW pattern is reversible for a change of heating current direction. A PSDW pattern as in series B disappears and transforms into the common step band pattern as in series A when heating current direction changes from

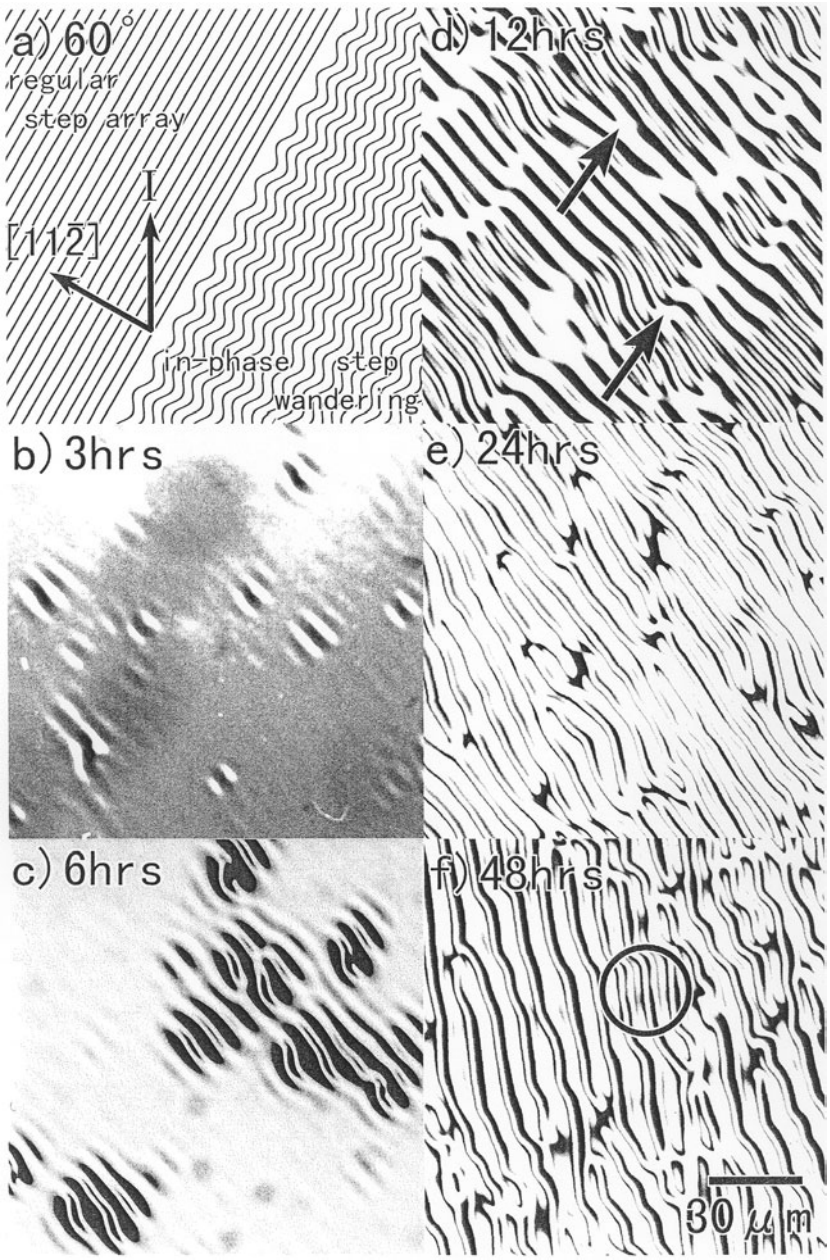

Figure 18. Optical micrographs which show time evolution of an IPSW when the dc direction was 60° from the step-down direction as schematically shown in panel (a). A delayed nucleation and growth of the IPSW (compare figures 18(b)–(d) with 12(a)–(c)) and reorientation of the direction of ridges and valleys from the step-down direction to the dc direction from (b)–(f) is noted.

the step-down to the step-up direction, and vice versa. Thus, the transition between the common step bunching pattern and the PSDW pattern is caused by a change of heating current direction. Although similar PSDW patterns were observed on the 1°, 2°, 5° and 7°-off vicinal surfaces

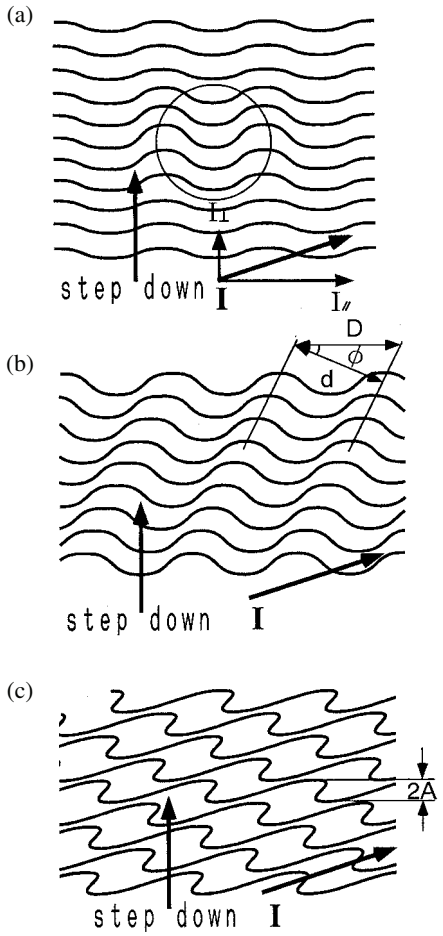

Figure 19. A schematic drawing of nucleation and reorientation of IPSW during dc heating, which occurs when the current direction is not parallel to the step-down direction. Heavily asymmetric wandering of individual steps is shown in (c) where ridges are parallel to the current.

inclined toward the $[11\bar{2}]$ direction, the PSDW pattern was not formed on the vicinal surface inclined toward the $[\bar{1}\bar{1}2]$ direction. The period of the PSDW pattern on the vicinal surface systematically depends on the off-angle and the substrate temperature; the period reduces to 50 nm and smaller periodic structure would be possible by optimization of experimental conditions [55]. Thus, application or expansion of this kind of composite technique might enable us to open a new technology of nano-structure fabrication by self-organization.

The fact that step bunching occurs either by step-up or step-down current heating as shown in series A and B means that step bunching is not due to the kinetic effect of electromigration of Si adatoms but due to the thermodynamic effect of Au adsorption. The fact that step bunching occurs with ac heating of 50 Hz as in (a) also supports this conclusion [7]. The driving force of step bunching must be a decrease of the free energy of the Si(111) surface by Au adsorption [56, 57] as in the case of Au/Si(001) or Cu/Si(111) [58–63]. On the other hand the fact that patterns formed under the step-up and step-down heating conditions are quite different suggests different step structure depending on the heating current direction.

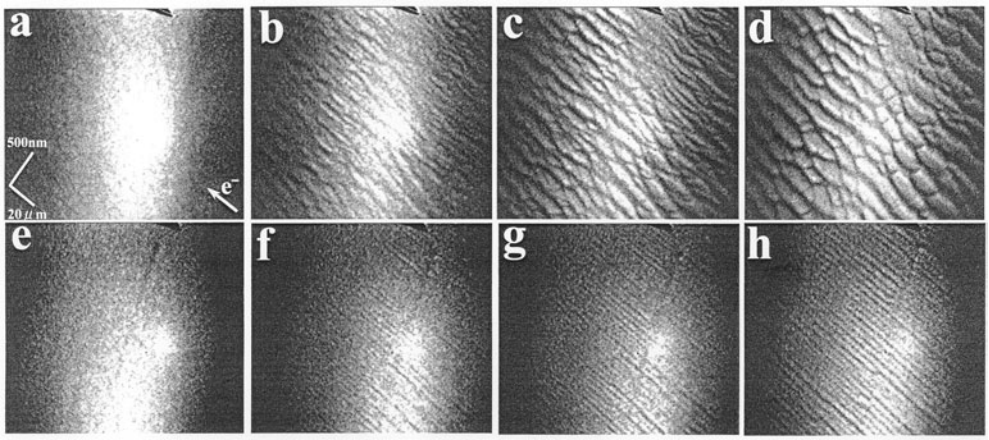

Figure 20. Two series of REM images showing step bunching during the deposition of Au on a 5°-off Si(111) vicinal surface at 860 °C. Heating current direction is in the step-up direction for series A ((a)–(d)) and in the step-down direction for series B ((e)–(h)). Adsorption rate of Au was about 0.1 ML min^{-1} and deposition times for (a)–(d) are 173, 193, 197 and 218 s and (e)–(h) 172, 175, 179 and 182 s respectively.

In series A, widths of step bands or (111) terraces vary from place to place in the case of the common step bunching process. Coarsening of the step bands is seen in series A and step bands are not straight and many branches of step bands are formed. On the other hand the coarsening of the step bands does not occur during PSDW formation as seen in series B. The step bands and the (111) terraces are quite straight and hardly any branches of step bands are seen. The periods of the patterns are almost constant in all the bunching stages; the slight increase is less than 15%. The time evolution of terrace width between adjacent step bands along the $[11\bar{2}]$ direction was found to be that the (111) terrace grows as $t^{1/2}$ for step-up current heating and it grows as $t^{1/4}$ for step-down current. These time evolutions do not depend on the deposition rate of Au, the substrate temperature or the off-angle of the vicinal surface. From the theoretical study of spinodal decomposition that discusses time evolution of characteristic size of the system [64], the power law factor $1/4$ shows the local mass transport case and $1/2$ shows the non-local mass transport case. In the case of Au on the Si(001) vicinal surface permeability of steps for Si adatoms depends on the substrate temperature [59]. In the case of PSDWs Si mass transport is local or steps are impermeable for Si adatoms, and it is non-local or steps are permeable for Si adatoms in the case of the usual step bunching. Step permeability for Si adatoms changes when the heating current direction is changed: for step-up current heating steps are permeable and for step-down current heating they are impermeable. This suggests again that step structure changes on changing heating current direction.

The reason for different step structure depending on the heating current direction is attributed to the effect of surface electromigration of Au atoms. Au atoms migrate to the anode [65] and the preferential migration direction is anti-parallel to the current directions shown in figure 21. A higher activation barrier for diffusion exists at steps [66, 67]. Thus, the Au adatoms tend to decorate the lower side of the steps for the step-down direction and the upper side of the steps for the step-up direction. Thus the step structure should be differently modified depending on the heating current direction.

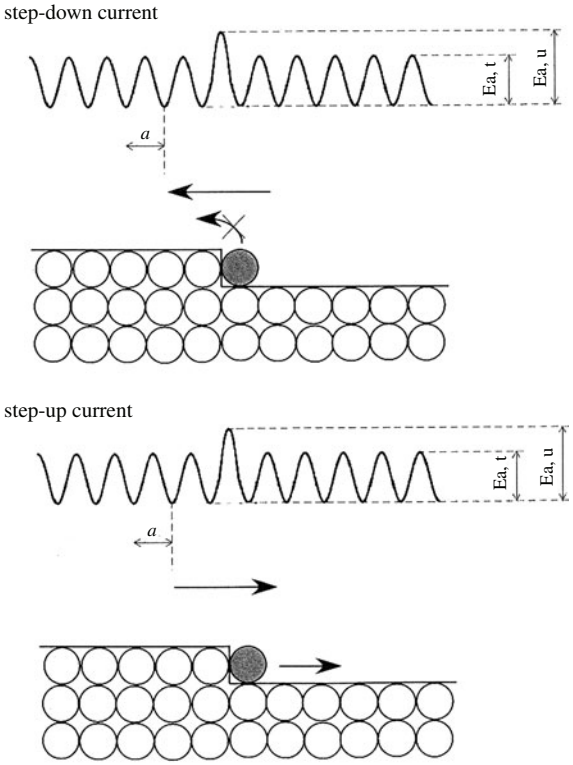

Figure 21. Schematic drawing showing the different step structures depending on the heating current direction.

5. Summary

5.1. IPSWs

Step instabilities due to dc-heating effects on a clean Si(111) 1×1 vicinal surface were studied. Complicated phase transitions of step configuration due to dc-heating effects occur for vicinal surfaces with large off-angle. However, the transition temperature depends on the off-angle of the vicinal surfaces. The transition temperature between ranges I and II decreases and that between ranges II and III increases with increasing off-angle.

Our recent study shows that the effective charge of the Si adatoms is positive in temperature ranges I–III, and this suggests that transition occurs by a change of the mechanism of step instability. The only explanation that gives a transition of step configuration seems to be the change of the permeability of steps for Si adatoms. The change of the step permeability modifies the relationship between step configuration and direction of the heating current and the phase transition takes place. Within this framework the fact that the transition temperature depends on the off-angle of the vicinal surface shows that step permeability depends on off-angle or step density. At present there is no clear explanation for this dependence. The fact that the wandering pattern propagates through the step–step interaction as described below might be a reason for the off-angle dependent transition temperature for the step-down current heating case. On the vicinal surface with a large off-angle the wandering pattern easily propagates and the temperature range at which IPSWs occur would be wider. However, this could not be

applicable for the step-up current heating case. Further investigations are needed to elucidate the origin of the transition.

We found the IPSW instability induced by the dc-heating effect in temperature range II. From the investigations of time evolution of the IPSW, we found the following.

(1) The growth processes are divided into three: (1) nucleation; (2) expansion; (3) propagation.

(2) Time evolutions of the periods or wavelengths and amplitudes on various kinds of vicinal surface were investigated and it was found that amplitudes initially grow as $t^{1/2}$ and saturate after 24–48 h, and the period does not depend on the annealing time or the off-angle of the vicinal surface. This finding on the period is one of the most important findings. This suggests that the period is a very good observable for future quantitative studies on IPSWs and dc-heating effects on the vicinal surface.

(3) The effect of the drift force component parallel to the mean step direction ($I_{\parallel}$) was investigated. The results show that the nucleation process was not greatly affected by $I_{\parallel}$, and the propagation of the wandering pattern is through the step–step repulsive interaction. Thus, the direction of the wandering pattern is inclined toward the step normal direction, not the heating current direction. The effect of $I_{\parallel}$ becomes larger and the pattern is inclined toward the heating current direction at the later stage of the growth.

5.2. PSDWs

The dynamics of the step bunching on the Si(111) vicinal surfaces induced by Au adsorption have been studied by REM. Steps are bunched by thermodynamics or Au adsorption irrespective of the heating current direction above the critical coverage of Au deposition (0.3 ML). Although step bunching occurs irrespective of the heating current direction, patterns after step bunching depend on the heating current direction and the PSDW was formed under the step-down current heating condition. The PSDW is the bunching pattern where extremely straight steps and (111) terraces are periodically arranged and is only observed by a combination of metal adsorption and the dc-heating effect. Quantitative analysis of time evolution of the width of a Si(111) terrace showed that widths grow as $t^{1/4}$ for step-down current heating and as $t^{1/2}$ for step-up current heating. These results show that mass transport kinetics of Si adatoms as well as the pattern depends on the heating current direction; steps are permeable for Si adatoms for step-up current heating and impermeable for Si adatoms for step-down current heating. These properties of steps depending on the heating current direction suggest that the atomic structure of the steps depends on the heating current direction.

Acknowledgments

Part of the study described in the present paper was performed in collaboration with Professor Yagi, Mr Y Tanishiro and Mr M Degawa at the Tokyo Institute of Technology and Professor E D Williams and Dr K Thurmer at the University of Maryland. The author would like to thank them for their help. The author would also like to thank Professor A Natori at the University of Electro-Communication, M Uwaha at Nagoya University, Professor Y Saito at Keio University and Professor J Weeks and Dr D J Liu at Maryland University for fruitful discussions. These studies were financially supported by a Grant-in Aid from the Ministry of Education, Science, Sports and Culture of Japan (grant No 09NP1001).

References

[1] Jeong H-C and Williams E D 1999 *Surf. Sci. Rep.* **34** 171 and references therein
[2] Yagi K, Minoda H and Degawa M 2001 *Surf. Sci. Rep.* **43** 45 and references therein
[3] Latyshev A V, Assev A L, Krasilnikov A B and Stenin S I 1989 *Surf. Sci.* **213** 157
[4] Degawa M, Nishimura H, Tanishiro Y, Minoda H and Yagi K 1999 *Japan. J. Appl. Phys.* **38** L308
[5] Homma Y and Aizawa N 2000 *Phys. Rev.* B **62** 8323
[6] Yamaguchi H and Yagi K 1993 *Surf. Sci.* **298** 408
[7] Yasunaga H and Natori A 1992 *Surf. Sci. Rep.* **15** 205 and references therein
[8] Zhou Z M, Baba S and Kinbara A 1982 *Thin Solid Films* **98** 109
[9] Yamanaka A, Yagi K and Yasunaga H 1989 *Ultramicroscopy* **29** 161
[10] Yagi K, Yamanaka A and Yamaguchi H 1993 *Surf. Sci.* **283** 300
[11] Yamanaka A, Tanishiro Y and Yagi K 1992 *Surf. Sci.* **264** 55
[12] Yamanaka A, Tanishiro Y and Yagi K 1992 *Ordering at Surfaces and Interfaces* (*Springer Series in Materials Science* vol 17) ed A Yoshimori, T Shinjo and H Watanabe (Berlin: Springer) p 215
[13] Kono S, Goto T, Ogura Y and Abukawa T 1999 *Surf. Sci.* **420** 240
[14] Yamaguchi H, Ohkawa T and Yagi K 1993 *Ultramicroscopy* **52** 306
[15] Stoyanov S 1991 *Japan. J. Appl. Phys.* **30** 1
[16] Natori A 1994 *Japan. J. Appl. Phys.* **33** 3583
[17] Saito Y and Uwaha M 1996 *J. Phys. Soc. Japan* **65** 3576
[18] Sato M and Uwaha M 1997 *J. Phys. Soc. Japan* **66** 1054
[19] Uwaha M and Sato M 1998 *Surf. Rev. Lett.* **5** 841
[20] Liu D-J and Weeks J D 1998 *Phys. Rev.* B **57** 14891
[21] Sato M and Uwaha M 1999 *Surf. Sci.* **442** 318
[22] Kandel D and Kaxiras E 1996 *Phys. Rev. Lett.* **76** 114
[23] Natori A, Suzuki T and Yasunaga H 1996 *Surf. Sci.* **367** 56
[24] Takeuchi N, Selloni A and Tossatti E 1994 *Phys. Rev. Lett.* **72** 2227
[25] Homma Y, Hibino H, Ogino T and Aizawa N 1997 *Phys. Rev.* B **55** R10237
[26] Stoyanov S 1997 *Surf. Sci.* **370** 345
[27] Stoyanov S and Tonchev V 1998 *Phys. Rev.* B **58** 1590
[28] Stoyanov S 1998 *Surf. Sci.* **416** 200
[29] Suga N, Kimbara J, Wu N-J, Yasunaga H and Natori A 2000 *Japan. J. Appl. Phys.* **39** 4412
[30] Fujita K, Ichikawa M and Stoyanov S 1999 *Phys. Rev.* B **60** 16006
[31] Sato M and Uwaha M 1997 *J. Phys. Soc. Japan* **65** 2146
[32] Sato M, Uwaha M and Saito Y 1998 *Phys. Rev. Lett.* **80** 4233
[33] Degawa M, Minoda H, Tanishiro Y and Yagi K 2000 *Surf. Sci.* **461** L258
[34] Degawa M, Minoda H, Tanishiro Y and Yagi K 2001 *Phys. Rev.* B **63** 045309
[35] Degawa M, Thurmer K, Morishima I, Minoda H, Yagi K and Williams E D 2001 *Surf. Sci.* **487** 171
[36] Degawa M, Minoda H, Tanishiro Y and Yagi K 2001 *J. Phys. Soc. Japan* **70** 1026
[37] Minoda H, Morishima I, Degawa M and Yagi K 2001 *Surf. Sci.* **493** 487
[38] Degawa M, Minoda H, Tanishiro Y and Yagi K 1999 *Surf. Rev. Lett.* **6** 977
[39] Nishimura H, Minoda H, Tanishiro Y and Yagi K 1999 *Surf. Sci.* **442** L1006
[40] Degawa M, Minoda H, Tanishiro Y and Yagi K 1999 *J. Phys.: Condens. Matter* **11** L551
[41] Minoda H 2003 submitted
[42] Latyshev A V, Minoda H, Tanishiro Y and Yagi K 1998 *Appl. Surf. Sci.* **130–132** 60
[43] Latyshev A V, Minoda H, Tanishiro Y and Yagi K 1998 *Surf. Sci.* **401** 22
[44] Minoda H 2001 *Phys. Rev.* B **64** 23305
[45] Minoda H 2002 *J. Phys. Soc. Japan* **71** 2944
[46] Kondo Y, Yagi K, Kobayashi K, Yanaka H, Kise Y and Ohkawa T 1991 *Ultramicroscopy* **36** 142
[47] Yagi K 1993 *Surf. Sci. Rep.* **17** 305
[48] Bales G S and Zangwill Z 1990 *Phys. Rev.* B **41** 5500
[49] Sato M, Uwaha M and Saito Y 2000 *Phys. Rev.* B **62** 8452
[50] Latyshev A V, Krasilnikov A B and Aseev A L 1994 *Surf. Sci.* **311** 395
[51] Thuermer K, Liu D-J, Williams E D and Week J D 1999 *Phys. Rev. Lett.* **83** 5531
[52] Senoh T, Minoda H, Tanishiro Y and Yagi K 1996 *Surf. Sci.* **357/358** 518
[53] Homma Y and Aizawa N 2000 *Phys. Rev.* B **62** 8323
[54] Natori A and Suga N 2002 *Appl. Surf. Sci.* **190** 96
[55] Minoda H, unpublished

[56] Aoki K, Suzuki T, Minoda H, Tanishiro Y and Yagi K 1998 *Surf. Sci.* **408** 101
[57] Aoki K, Minoda H, Tanishiro Y and Yagi K 1998 *Surf. Rev. Lett.* **5** 653
[58] Minoda H, Yagi K, Meyer zu Heringdorf F-J, Meire A, Koeler D and Horn von Hoegen M 1999 *Phys. Rev.* B **59** 2363
[59] Minoda H and Yagi K 1999 *Phys. Rev.* B **60** 2715
[60] Minoda H, Shimakura T, Yagi K, Meyer zu Heringdorf F-J, Meire A, Koeler D and Horn von Hoegen M 2000 *Phys. Rev.* B **61** 5672
[61] Minoda H and Yagi K 1999 *Surf. Sci.* **437** L761
[62] Minoda H, Takahashi Y, Tanishiro Y and Yagi K 1999 *Surf. Sci.* **438** 68
[63] Takahashi Y, Minoda H, Tanishiro Y and Yagi K 1999 *Surf. Sci.* **433–435** 512
[64] Bray A J 1993 *Physica* A **194** 41
[65] Yasunaga H and Sasuga E 1990 *Surf. Sci.* **231** 263
[66] Kodiyalam S, Khor K E and Sarma S D 1996 *Phys. Rev.* B **53** 9913
[67] Kodiyalam S, Khor K E and Sarma S D 1996 *J. Vac. Sci. Technol.* B **14** 2817